

# Two-dimensional superconductivity at a Mott-Insulator/Band-Insulator interface : LaTiO<sub>3</sub>/SrTiO<sub>3</sub>

J. Biscaras<sup>1</sup>, N. Bergeal<sup>1</sup>, A. Kushwaha<sup>2</sup>, T. Wolf<sup>1</sup>, A. Rastogi<sup>2</sup>, R.C. Budhani<sup>2,3</sup> and J. Lesueur<sup>1</sup>

<sup>1</sup>*LPEM- UMR8213/CNRS - ESPCI ParisTech, 10 rue Vauquelin - 75005 Paris*

<sup>2</sup>*Condensed Matter - Low Dimensional Systems Laboratory, Department of Physics,  
Indian Institute of Technology Kanpur, Kanpur 208016, India and*

<sup>3</sup>*National Physical Laboratory, New Delhi - 110012, India.*

(Dated: 23 février 2024)

Transition metal oxides display a great variety of quantum electronic behaviours where correlations often play an important role. The achievement of high quality epitaxial interfaces involving such materials gives a unique opportunity to engineer artificial structures where new electronic orders take place. One of the most striking result in this area is the recent observation of a two-dimensional electron gas at the interface between a strongly correlated Mott insulator LaTiO<sub>3</sub> and a band insulator SrTiO<sub>3</sub> [1, 2]. The mechanism responsible for such a behaviour is still under debate. In particular, the influence of the nature of the insulator has to be clarified. Here we show that despite the expected electronic correlations, LaTiO<sub>3</sub>/SrTiO<sub>3</sub> heterostructures undergo a superconducting transition at a critical temperature  $T_c^{\text{onset}} \sim 300$  mK. We have found that the superconducting electron gas is confined over a typical thickness of 12 nm. We discuss the electronic properties of this system and review the possible scenarios.

Perovskites based structures including transition metal oxides have attracted much attention in the last decades, with the discovery of high- $T_c$  superconductivity and colossal magnetoresistance [3]. More generally, these compounds exhibit various electronic orders, going from the canonical Anti-Ferromagnetic (AF) Mott insulator when the on-site repulsion is maximum because of strong

electronic interactions, to Fermi Liquid like metals when carrier doping is such that screening prevents the system from localisation. Depending on the cations and the doping level involved, charge, spin and orbital orders can appear in the ground state together with metallic and even superconducting phases. Transitions between these states can be tuned by temperature, magnetic or electric fields [4]. All these compounds can be seen as stacks of oxide layers where the charge neutrality is conserved in the unit cell, but not necessarily in each layer. Therefore, the translation symmetry is locally broken at the interface and charge imbalance can develop. Like in band gap engineering with semiconductors, it is possible to create artificial interface materials by growing thin layers of a transition metal oxide on top of another one. Recently, the observation of two-dimensional superconductivity and magnetic correlations [5] at the interface between the two band insulators  $\text{LaAlO}_3$  and  $\text{SrTiO}_3$  [6] has drawn a lot of attention. An other particularly interesting candidate is the homo-metallic structure  $\text{LaTiO}_3/\text{SrTiO}_3$  that uses  $\text{TiO}_2$  plans as a building block [2]. Titanium is in the  $3d^0$  state in the  $\text{SrTiO}_3$  layer which is a band insulator of 3.2 eV bandgap, while it is  $3d^1$  in the  $\text{LaTiO}_3$  one which is therefore an AF Mott insulator due to strong correlations [7]. Providing the interface layer is  $\text{TiO}_2$ , an extra electron is left in the structure every two unit cells [8, 12]. As shown by photoemission [9] and optical studies [10], a two-dimensionnal electron gas (2-DEG) develops and extends a few unit cells beyond the interface.

Several theoretical approaches pointed out that an electronic reconstruction leads to an increase of the electronic density at the  $\text{LaTiO}_3/\text{SrTiO}_3$  interface [8, 11–13]. Okamoto and Millis proposed a phase diagram where different orbital and magnetic states occur as a function of the thickness of the  $\text{LaTiO}_3$  layer and the strength of the Mott-Hubbard parameter  $U/t$  ( $U$  is the Coulomb on-site repulsion energy, and  $t$  the hopping term between neighbour Ti sites)[8]. Fully polarized ferromagnetic metallic sub-bands are expected to form for thickness below five unit cells and  $U/t \sim$

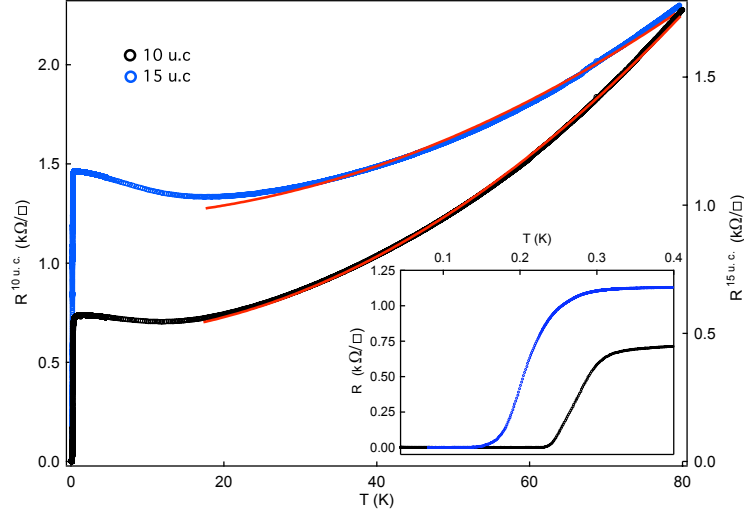


FIGURE 1: Sheet resistance  $R$  of the 10 u.c. (left axis) and 15 u.c. (right axis)  $\text{LaTiO}_3/\text{SrTiO}_3$  samples in an intermediate range of temperature. The red lines correspond to quadratic fits of the form  $R(T) = AT^2 + R_0$ . Inset ) Sheet resistance as a function of temperature showing the superconducting transitions at  $T_c^{\text{onset}} \approx 310 \text{ mK}$  for the 10 u.c. and  $T_c^{\text{onset}} \approx 260 \text{ mK}$  for the 15 u.c., where  $T_c^{\text{onset}}$  is defined by a 10% drop of the resistance.

8 – 10. On the other hand Kancharla and Dagotto [14] taking into account both local and long range Coulomb interactions, showed that strong AF fluctuations reminiscent of the magnetic order of the bulk compound persist in the metallic phase. As suggested by Larson [15] and Okamoto [16], lattice relaxation at the interface strongly modifies the band configuration, and may enhance the electronic correlations in the 2-DEG [11]. In this context, it is clear that the  $\text{LaTiO}_3/\text{SrTiO}_3$  interface layer appears to be a unique system to study the physics of a 2-DEG influenced by strong electronic correlations.

We have grown epitaxial layers of  $\text{LaTiO}_3$  using excimer laser based Pulsed Laser Deposition (PLD) on single crystal substrates of  $\text{SrTiO}_3$  cut along (100) and (110) crystallographic directions. The details of the growth conditions and X-rays characterisations are given in Supplementary Information. In this study, we focus mainly on two  $\text{LaTiO}_3/(100)\text{SrTiO}_3$  hetero-structures whose thickness of 40 Å and 60 Å correspond to 10 and 15 unit cells (u.c.) respectively. The sheet

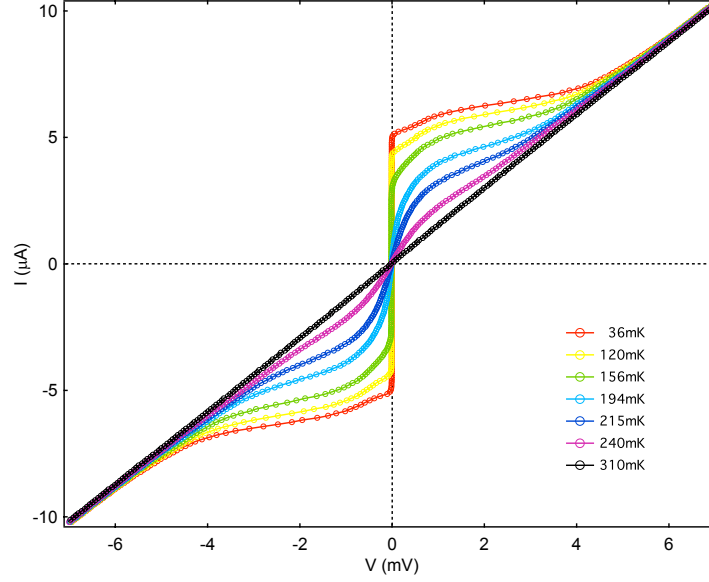


FIGURE 2: Current-voltage characteristics of the 10 u.c. sample at different temperatures. The critical current at low temperature is  $5 \mu\text{A}$  corresponding to a critical current per unit width of  $16.7 \mu\text{A}/\text{cm}$ .

resistance measured in a Van-der-Pauw geometry decreases with temperature, indicating a metallic behaviour of the interface (figure 1). At temperatures lower than 20K the two samples exhibit an increase of resistance characteristic of weak localisation in disordered two-dimensional films. The hetero-structures undergo a superconducting transition at  $T_c^{\text{onset}} \approx 310 \text{ mK}$  for the 10 u.c. sample and at  $T_c^{\text{onset}} \approx 260 \text{ mK}$  for the 15 u.c. sample (inset figure1). Thinner 5 u.c. (100) films and 20 to 100 u.c. thicker (100) films as well as (110) oriented films are not metallic at low temperature.

In figure 2, we show the current-voltage characteristics of the 10 u.c. sample measured at different temperatures. At low temperature, the  $I(V)$  curves displays a clear critical current  $I_c$  of  $5 \mu\text{A}$  corresponding to a critical current per unit width of  $16.7 \mu\text{A}/\text{cm}$ . For current much higher than  $I_c$ , the  $I(V)$  curves merge together on a linear Ohmic law with a resistance corresponding to the normal resistance. In the case of the 15 u.c. sample, the critical current per unit width is found to be  $14 \mu\text{A}/\text{cm}$ . Figure 3a shows the sheet resistance of the 10 u.c sample as a function of

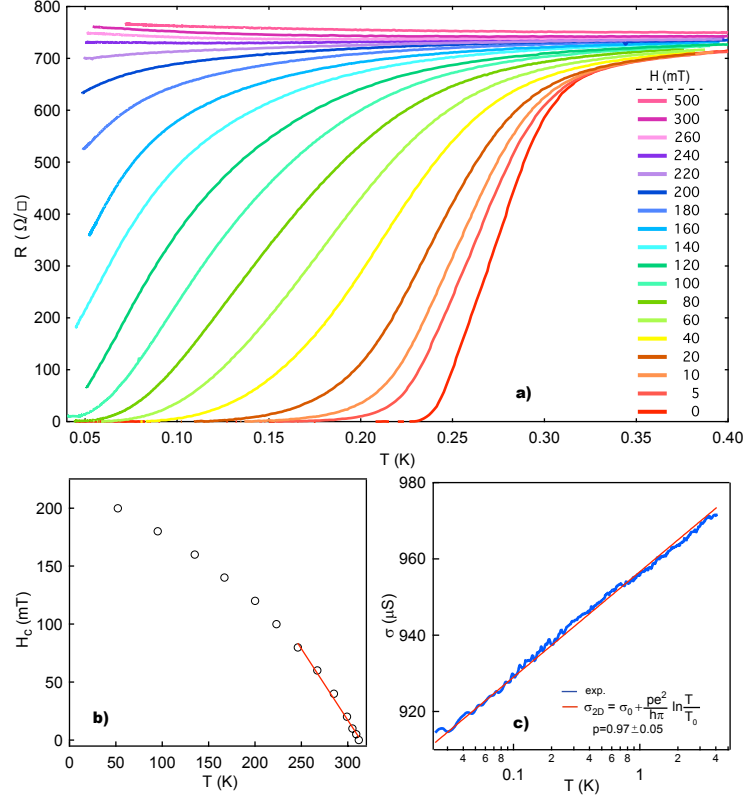


FIGURE 3: a) Sheet resistance of the 10 u.c. sample as a function of temperature for different values of the perpendicular magnetic field. b) Temperature dependence of the perpendicular critical field, defined as the magnetic field that suppresses 90% of the resistance drop. The red line indicates the linear dependence of the critical field with temperature close to  $T_c$ . c) Conductivity of the 15 u.c. sample as a function of temperature for a perpendicular magnetic field corresponding to the critical field. The red line corresponds to the expression  $\sigma_{2D}(T) = \sigma_0 + \frac{pe^2}{\pi h} \ln \frac{T}{T_0}$  with  $p = 0.97$  indicating that phase coherence is limited by electron-electron scattering ( $p=1$ )[19].

temperature measured for different values of a magnetic field applied perpendicularly to the sample. The magnetic field induces a transition from a superconducting state to a non-superconducting one. The dependence of the critical field as a function of temperature is linear close to  $T_c$ , which is consistent with the form  $H(T) = \frac{\Phi_0}{2\pi\xi_{\parallel}^2(T)}$  taking into account a Landau-Ginsburg in-plane coherence length  $\xi_{\parallel} \propto (T_c - T)^{-\frac{1}{2}}$  (figure 3b). The critical field extrapolated at  $T=0$  is  $H_{\perp}^c \approx 220$  mT for the 10 u.c. sample and  $H_{\perp}^c \approx 210$  mT for the 15 u.c. sample (see supplementary figure 3). At  $T=0$ , we found  $\xi_{\parallel}^{10u.c.}(T=0) \approx 38$  nm and  $\xi_{\parallel}^{15u.c.}(T=0) \approx 42$  nm. Measurements performed in a

parallel magnetic field geometry give  $H_{\parallel}^c = \frac{\sqrt{3}\Phi_0}{\pi d\xi_{\parallel}(T=0)} \approx 2.15$  T for the 10 u.c sample and  $H_{\parallel}^c=2.2$  T for the 15 u.c sample. We thus extract the thickness of the two-dimensional superconducting electron gas  $d^{15u.c.} \approx 12$  nm and  $d^{10u.c.} \approx 13.5$  nm. Note that this is an upper bound given the precision of the sample alignment in the parallel magnetic field. These values are closed to the ones reported in  $\text{LaAlO}_3/\text{SrTiO}_3$  hetero-structures[17, 18]. In disordered electronic system, weak localisation produces a decrease of conductivity that can be experimentally revealed by varying the temperature. In the particular case of a two-dimensional system, the conductivity takes the remarkable logarithmic dependence with temperature  $\sigma_{2D}(T) = \sigma_0 + \frac{pe^2}{\pi h} \ln \frac{T}{T_0}$  where  $p$  depends on the process that limits the phase coherence.  $p = 3$  for electron-phonon scattering and  $p = 1$  for electron-electron scattering in the dirty limit[19]. Such logarithmic temperature dependence is observed on our samples (see figure 3c), thus confirming the two-dimensional nature of the electron gas. The fit gives  $p = 0.97 \pm 0.05$  showing that the phase coherence is limited mainly by electron-electron scattering.

It is known that  $\text{LaTiO}_3$  itself can be oxygen [20–22] or Sr doped [23], and thus becomes metallic. The key question is therefore : does superconductivity take place within a doped Mott insulator layer, namely oxygen or Sr doped  $\text{LaTiO}_3$ , or within a 2-DEG formed at the  $\text{LaTiO}_3/\text{SrTiO}_3$  interface, which extends mostly within the band insulator  $\text{SrTiO}_3$  [8]? And conversely, do the electronic correlations, which are known to be strong in the former case and moderate in the latter one[16], play a role in that context? The recent works on  $\text{LaTiO}_3/\text{SrTiO}_3$  superlattices [2, 10, 24] clearly indicate that under proper growth conditions, the interface is abrupt, with no sizable Sr diffusion for deposition temperatures below 1000 °C[9]. Optical spectroscopy confirms that the carrier properties in superlattices are different than the ones in  $\text{La}_{1-x}\text{Sr}_x\text{TiO}_3$  compounds [10]. Moreover, the low temperature transport properties are different in conducting doped  $\text{LaTiO}_3$  and

doped SrTiO<sub>3</sub>. In both cases, electron-electron collisions dominate the scattering events according to the Fermi liquid picture. Figure 1 shows that, in an intermediate regime temperature, the temperature dependence of the resistance is well fitted by a quadratic law  $R(T) = AT^2 + R_0$  where the coefficient  $A$  depends on the Landau parameters, and therefore on the carrier density and the effective mass  $m^*$ [25]. We obtained  $A=0.27 \text{ } \Omega/\square K^2$  for the 10 u.c. sample and  $B=0.11 \text{ } \Omega/\square K^2$  for the 15 u.c. sample. In table [1] we summarise the different values of  $A$  found in the literature for doped LaTiO<sub>3</sub> and doped SrTiO<sub>3</sub> thin films and crystals and compare them to the values extracted from our experiment. The largest value of  $A$  reported in doped LaTiO<sub>3</sub> are on the order of  $1 \times 10^{-9} \Omega cm/K^2$  before the system becomes insulating at low temperature ( $\partial R/\partial T < 0$  for  $T < 100$  K), whereas it is two orders of magnitude higher for doped SrTiO<sub>3</sub>. From the comparison, we see that the LaTiO<sub>3</sub>/SrTiO<sub>3</sub> interface layer behave more like doped SrTiO<sub>3</sub> than doped LaTiO<sub>3</sub>. This indicates that the 2-DEG extends mostly in the SrTiO<sub>3</sub> substrate and makes it conducting [8].

To investigate the density and mobility of charge carriers, we have performed Hall measurements at low temperature (figure 4). The experiment confirms that the sign of the hall coefficient  $R_H = \frac{V_H}{IB}$  is negative for both samples, indicating that electron-like charge carriers dominate the transport. The sheet carrier density  $n_S = \frac{1}{eR_H}$  was found to be  $2 \times 10^{14} cm^{-2}$  for the 10 u.c. sample and  $= 2.7 \times 10^{13} cm^{-2}$  for the 15 u.c. one. Taking the sheet resistance measured previously, we obtained a Hall mobility  $\mu = \frac{1}{eR_s n_s}$  of  $52 \text{ } cm^2 V^{-1} s^{-1}$  for the 10 u.c. sample and  $210 \text{ } cm^2 V^{-1} s^{-1}$  for the 15 u.c. one. In an ideal picture, the interface between SrTiO<sub>3</sub> and LaTiO<sub>3</sub> can be seen as a Ti ions network, in the  $4^+$  state in SrTiO<sub>3</sub> and in the  $3^+$  one in LaTiO<sub>3</sub>. Therefore, one electron is left every two cells on average at the interface, which corresponds to an areal density of around  $3 \times 10^{14} cm^{-2}$  [8, 12]. This is approximatively the electron density measured through Hall effect in the 10 u.c. sample ( $2 \times 10^{14} cm^{-2}$ ), consistent with the value observed in LaTiO<sub>3</sub>/SrTiO<sub>3</sub> superlattices [2] by

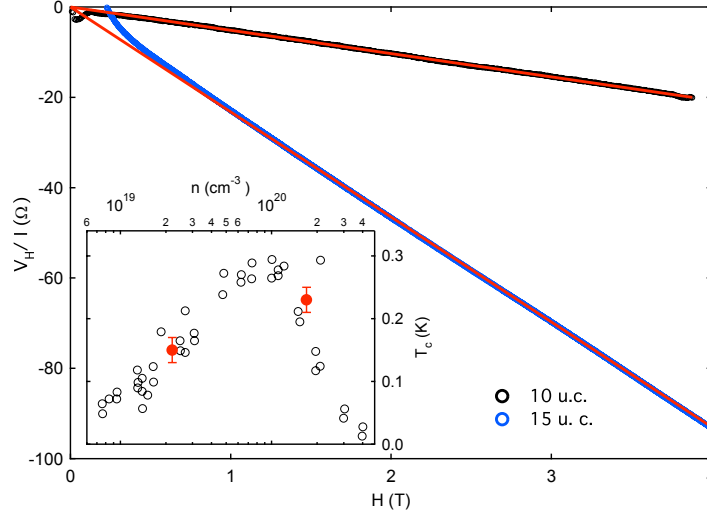


FIGURE 4: a) Hall voltage  $V_H$  divided by the current  $I$  as a function of magnetic field for the 10 u. c. and 15 u.c.  $\text{LaTiO}_3/\text{SrTiO}_3$  samples, measured at 100 mK. Red solid lines correspond to linear fits. Inset)  $T_c$  as a function of doping for  $\text{SrTiO}_3$  single crystals taken from [27] (black open circles). The two red dots corresponds to  $\text{LaTiO}_3/\text{SrTiO}_3$  samples taking the thickness  $d^{10\text{u.c.}} \approx 12$  nm,  $d^{15\text{u.c.}} \approx 13.5$  nm. Here, we have defined  $T_c$  as the temperature at which the resistance reaches zero since this definition is more appropriate for comparison with the magnetic definition of the  $T_c$  used in reference [27].

measuring the number of  $\text{Ti}^{3+}$  in the vicinity of the interface. Optical studies confirm that free carriers with densities of around  $3 \times 10^{14}/\text{cm}^2$  do exist in similar superlattices, with a typical mobility of  $35 \text{ cm}^2/\text{Vs}$  and an effective mass  $m^* \simeq 2m_e$  [10]. The mobility that we measured on the 10 u.c. sample ( $52 \text{ cm}^2/\text{Vs}$ ) is close to this value, which supports an effective mass close to  $2m_e$ . The 15 u.c. has a lower sheet density of  $2.7 \times 10^{13}/\text{cm}^2$  and a  $T_c^{\text{onset}}$  of only 260 mK. These observations are consistent with an electronic reconstruction of the  $\text{LaTiO}_3/\text{SrTiO}_3$  interface, leading to the formation of a few unit cells thick 2-DEG in the  $\text{SrTiO}_3$  layer [8, 15, 16]. As shown in figure 4 inset, our data are consistent with the dependence of  $T_c$  with the carrier density reported in the literature of doped  $\text{SrTiO}_3$  [27].

In summary, we have measured the electronic transport properties of  $\text{LaTiO}_3/\text{SrTiO}_3$  heterostructures. The samples display a metallic behaviour and a superconducting transition is observed at



Compound	Ox. LaTiO <sub>3</sub> <sup>a</sup>	Sr. LaTiO <sub>3</sub> <sup>b</sup>	LaTiO <sub>3</sub> (10 u.c.)/SrTiO <sub>3</sub>	LaTiO <sub>3</sub> (15 u.c.)/SrTiO <sub>3</sub>	La. STO <sup>c</sup>	La. STO <sup>c</sup>
$A(\Omega cm/K^2)$	$8 \times 10^{-9}$	$2 \times 10^{-9}$	$3.6 \times 10^{-7}$	$1.3 \times 10^{-7}$	$5 \times 10^{-7}$	$3 \times 10^{-8}$

TABLE I: Comparison of  $A$  parameters (given in  $\Omega cm/K^2$ ) measured in the 10 u.c. and 15 u.c. LaTiO<sub>3</sub>/SrTiO<sub>3</sub> samples (taking the thickness  $d^{10u.c.}=12$  nm,  $d^{15u.c.}=13.5$  nm), with data obtained from literature on thin films and crystals for similar doping : <sup>a</sup> oxygen doped LaTiO<sub>3</sub> by Taguchi et al[20]; <sup>b</sup> Sr doped LaTiO<sub>3</sub> by Tokura et al[23]; <sup>c</sup> Two different La doped SrTiO<sub>3</sub> by Okuda et al[26].

low temperature. Our analysis shows that a 2-DEG is formed at the interface which extends mostly in the SrTiO<sub>3</sub> substrate, in agreement with the electronic reconstruction scenario[8]. This discovery opens the possibility to study the interplay between superconductivity and different electronic orders predicted to take place with ultra-thin LaTiO<sub>3</sub> films on SrTiO<sub>3</sub>. According to our results in terms of carrier density, mobility and gas thickness, it should be possible to modulate significantly the behaviour of the 2-DEG by adjusting the number of charge carriers with an electrostatic gate.

The authors acknowledge L. Benfatto, M. Grilli, S. Caprara, C. Castellani, C. Di Castro for useful discussions and L. Dumoulin for technical support.

- 
- [1] Ohtomo, A., Hwang, H. Y. A high-mobility electron gas at the LaAlO<sub>3</sub>/SrTiO<sub>3</sub>. Nature **427** 423-426 (2004).
  - [2] Ohtomo A., Muller, D. A., Grazul, J. L., Hwang, H. Y. Artificial charge-modulation in atomic-scale perovskite titanate superlattices. Nature **419** 378-380 (2002).
  - [3] Dagotto. E., Complexity in strongly correlated electronic systems. Science **309**, 257 (2005).
  - [4] Imada M., Fujimori A., Tokura Y. Metal-insulator transitions. Rev. Mod. Phys. **70**, 1039 (1998).
  - [5] Brinkman et al. Magnetic effects at the interface between non-magnetic oxides. Nature Mater. **6**, 494 (2007).
  - [6] Reyren, N. et al. Superconducting interfaces between insulating oxides. Science **317** 1196-1199 (2007).
  - [7] Tokura, Fillingness dependence of electronic-structures in strongly correlated electron-systems- titanates and vanadates. J. Phys. Chem. Solids **53**, 1619-1625, (1992).
  - [8] Okamoto, S., Millis, A. J. Electronic reconstruction at an interface between a Mott insulator and a band insulator. Nature

**428** 630-633 (2004).

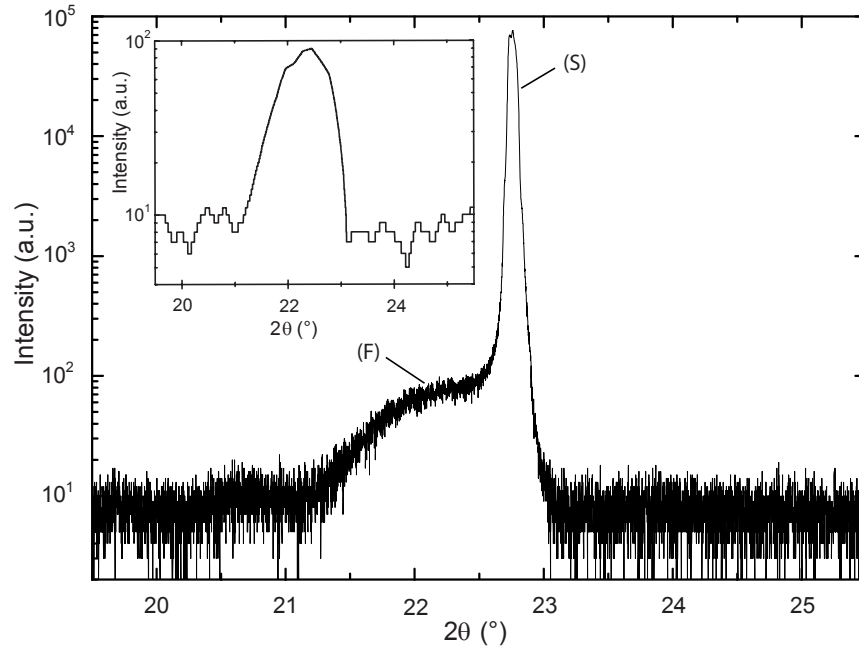
- [9] Takizawa, M. Photoemission from Buried Interfaces in  $\text{SrTiO}_3$  / $\text{LaTiO}_3$  Superlattices Phys. Rev. Lett. **97**, 057601 (2006).
- [10] Seo, S. S., Choi, W. S., Lee, H. N., Yu, L., Kim, K. W., Bernhard, C. Noh, T. W. Optical Study of the Free-Carrier Response of  $\text{LaTiO}_3$ / $\text{SrTiO}_3$  Superlattices. Phys. Rev. Lett. **99**, 266801 (2007).
- [11] Ishida, H., Liebsch A., Origin of metallicity of  $\text{LaTiO}_3$ / $\text{SrTiO}_3$  heterostructures. Phys. Rev. **77** 115350 (2008).
- [12] Okamoto, S., Millis, A. J. Spatial inhomogeneity and strong correlation physics : A dynamical mean-field study of a model Mott-insulator-band-insulator heterostructure. Phys. Rev. B **70**, 241104 (2004).
- [13] Popovic, Z., Satpathy, S. and Martin, R. M. Origin of the Two-Dimensional Electron Gas Carrier Density at the  $\text{LaAlO}_3$  on  $\text{SrTiO}_3$  Interface. Phys. Rev. Lett. **101**, 256801 (2008).
- [14] Kancharla, S. S., Dagotto, E. Metallic interface at the boundary between band and Mott insulators. Phys. Rev. B **74** 195427 (2006).
- [15] Larson P., Popović, Z., Satpathy, S. Lattice relaxation effects on the interface electron states in the perovskite oxide :  $\text{LaTiO}_3$  monolayer embedded in  $\text{SrTiO}_3$  . Phys. Rev. B, **77**, 245122 (2008).
- [16] Okamoto, S., Millis, A. J., Spaldin, N. A. Lattice Relaxation in Oxide Heterostructures :  $\text{LaTiO}_3$ / $\text{SrTiO}_3$  Superlattices. Phys. Rev. Lett. **97**, 056802 (2006).
- [17] M. Basletic et al., Mapping the spatial distribution of charge carriers in  $\text{LaAlO}_3$ / $\text{SrTiO}_3$ . Nature Mater. **7**, 621 (2008).
- [18] Copie. O, et al. Towards Two-Dimensional Metallic Behavior at  $\text{LaAlO}_3$ / $\text{SrTiO}_3$  Interfaces, Phys. Rev. Lett. **102**, 216804 (2009).
- [19] Lee, P. A., Ramakrishnan, T. V. Disordered electronic systems. Rev. Mod. Phys. **57**, 287-3317 (1985).
- [20] Taguchi, Y., Okuda, T., Ohashi, M., Murayama, C., Mri, N., Iye, Y., Tokura, Y. Critical behavior in  $\text{LaTiO}_{3+\delta/2}$  in the vicinity of antiferromagnetic instability. Phys. Rev. B **59**, 7917 (1999).
- [21] Wang F., Li, J., Wang, P, Zhu, X., Zhang, M. Effect of oxygen content on the transport properties of  $\text{LaTiO}_{3+\beta/2}$  thin films. J. Phys. : Condens. Matter, **18**, 5835-5847 (2006).
- [22] Gariglio, S., Seo, J. W., Fompeyrine, J., Locquet, J.-P., Triscone, J.-M. Transport properties in doped Mott insulator epitaxial  $\text{La}_{1-y}\text{TiO}_{3+\delta}$  thin films. Phys. Rev. B **63**, 161103 (2001).
- [23] Tokura, Y., Taguchi, Y., Okada, Y., Fujishima, Y., Arima, T., Kumagai, K., Iye. Y. Filling dependence of electronic properties on the verge of metalMott-insulator transition in  $\text{Sr}_{1-x}\text{La}_x\text{TiO}_3$ . Phys. Rev. Lett. **70**, 2126 (1993).
- [24] Shibuya, K., Ohnishi, T., Kawasaki, M., Koinuma H., Lippmaa, M. Metallic  $\text{LaTiO}_3$ / $\text{SrTiO}_3$  superlattice films on the  $\text{SrTiO}_3$ . Jap. J. Appl. Phys. **43**, L1178-L1180 (2004).
- [25] Nozières, P., and Pines, D. The theory of quantum liquids, Perseus Books, Cambridge, MA (1999).
- [26] Okuda, T., Nakanishi, K., Miyasaka, S., Tokura, Y. Large thermoelectric response of metallic perovskites :  $\text{Sr}_{1-x}\text{La}_x\text{TiO}_3$ . Phys. Rev. B **63**, 113104 (2001).

- [27] Koonce, C. S., Cohen, M. L., Schooley, J. F., Hosler, W. R., Pfeiffer, E. R. Superconducting Transition Temperatures of Semiconducting  $\text{SrTiO}_3$  . Phys. Rev. **163**, 380 (1967).

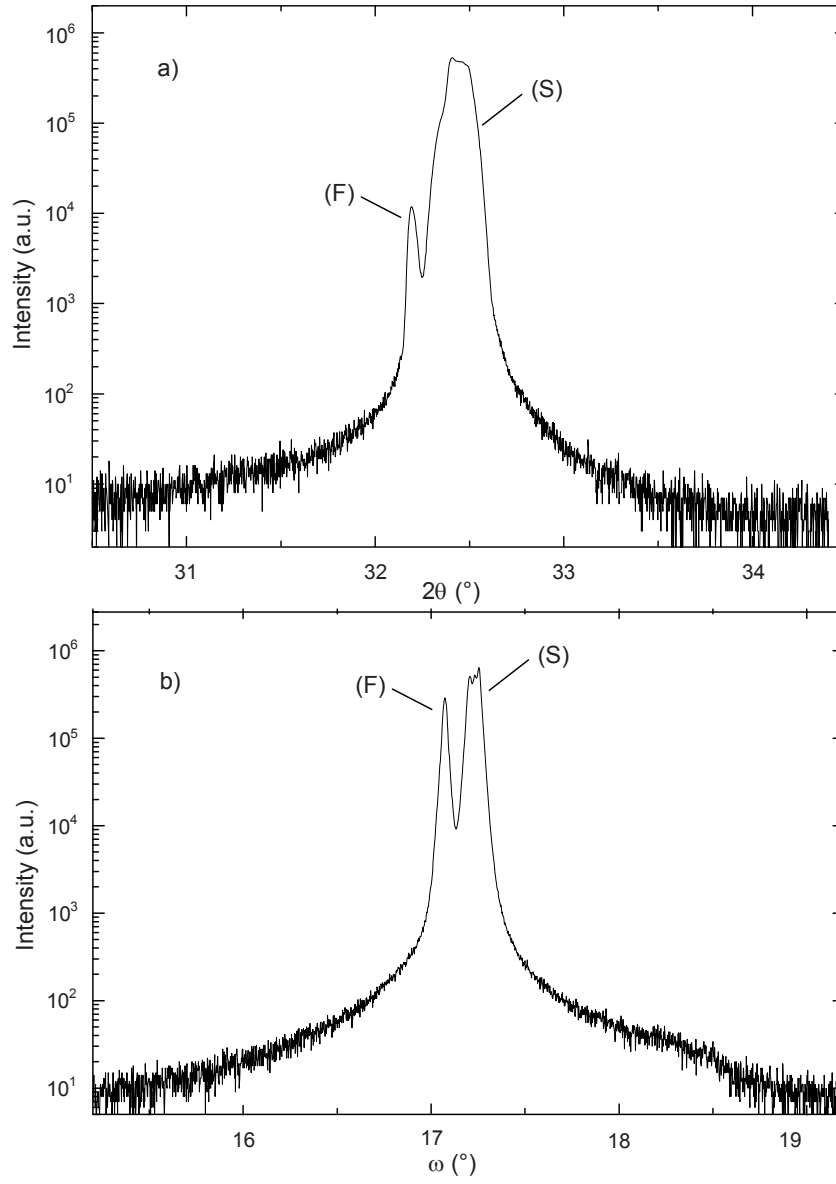
## Supplementary information

### Growth and characterization

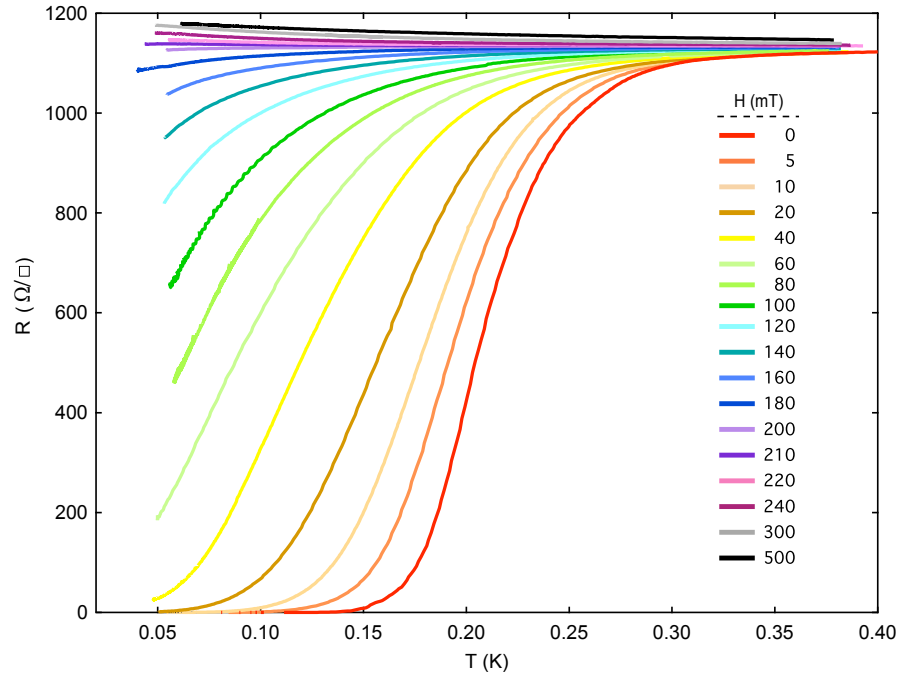
We have grown epitaxial layers of  $\text{LaTiO}_3$  using excimer laser based PLD on commercially available (Crystak gmbh Germany) single crystal substrates of  $\text{SrTiO}_3$  cut along (100) and (110) crystallographic directions. While the (100) substrates were given a buffered HF treatment to expose  $\text{TiO}_2$  terminated surface, the (110) plane has Sr, Ti and oxygen ions on one plane and hence HF treatment is irrelevant in this case. The substrates were glued to the heater block of the PLD system and heated in oxygen pressure of 200 mTorr in the temperature range of 850 to 950 °C for one hour to realize surface reconstruction. This process has been used routinely to grow epitaxial films and heterostructures of  $\text{YBa}_2\text{Cu}_3\text{O}_{6+x}$  and hole doped manganites. The source of  $\text{LaTiO}_3$  is a stoichiometric sintered target of 22 mm in diameter which was ablated in oxygen partial pressure of  $1 \times 10^{-4}$  Torr with energy fluence of  $\sim 1 \text{ J/cm}^2$  per pulse at a repetition rate of 3 Hz to realize a growth rate of 0.12 Å/s. Under these conditions, the  $\text{LaTiO}_3$  phase is grown on  $\text{SrTiO}_3$  substrates, as shown by X-Rays diffraction patterns. On (100) $\text{SrTiO}_3$ , a pure (100) $\text{LaTiO}_3$  film is grown (supplementary figure 1). On (110) $\text{SrTiO}_3$ , a pure (110) $\text{LaTiO}_3$  is observed (supplementary figure 2). In both cases, film peaks are almost aligned with the corresponding substrate ones, which confirms the good orientations.



Supplementary Figure 1. X-rays diffraction pattern ( $\theta - 2\theta$  scan) for  $\text{LaTiO}_3$  films (F) deposited on  $(100)\text{SrTiO}_3$  substrate. After subtracting the contribution of the substrate (S), the lattice parameter of the film is found to be  $3.956 \text{ \AA}$  (inset), in good agreement with previous studies [Havelia et al. *Journal of Crystal Growth* **310**, 1985 (2008)] and close to the one reported in bulk  $\text{LaTiO}_3$  ( $3.928 \text{ \AA}$ ) [Kestigian et al., *J. Am. Chem. Soc.* **76**, 6027 (1954)].



Supplementary Figure 2. a) X-rays diffraction pattern ( $\theta$ - $2\theta$  scan) around  $32^\circ$  of LaTiO<sub>3</sub> films deposited on SrTiO<sub>3</sub>(110). The (110) peak of the film (F) is observed at  $2\theta=32.193^\circ$ , close to the (110) peak of the substrate (S), which corresponds to a LaTiO<sub>3</sub> lattice parameter of 3.928 Å. b) X-rays diffraction rocking curve ( $\omega$  scan) of the (110) peak of LaTiO<sub>3</sub> films on SrTiO<sub>3</sub>(110). The typical width of the curve is around  $0.1^\circ$  showing a very good out-of-plane plane orientation of the layers.



Supplementary Figure 3. Sheet resistance of the 15 u.c. sample as a function of temperature for different values of the perpendicular magnetic field.